

Pressure–Volume Curve Does Not Predict Steady-State Lung Volume in Canine Lavage Lung Injury

John M. Downie, Arthur J. Nam, and Brett A. Simon

Department of Anesthesiology and Critical Care Medicine, Johns Hopkins Medical Institutions, Baltimore, Maryland

To better understand strategies for recruiting and maintaining lung volume in acute lung injury, we examined relationships between steady-state lung volume and cumulative cyclic recruitment/derecruitment volume history and the quasi-static pressure–volume curve, in an animal saline lavage lung injury model. Small-volume tidal pressure–volume loops performed after inflation from functional residual capacity demonstrated incremental, cyclic recruitment only if the peak pressure achieved exceeded the pressure at which the compliance increased (P_{flex}) on the pressure–volume curve, whereas loops performed after deflation from total lung capacity remained close to the envelope deflation curve. Recruitment continued to occur up to and beyond a peak inspiratory airway pressure of 40 cm H₂O, as demonstrated by both the tidal loops and by computed tomography-derived lung volume data. Tidal-specific compliance was relatively constant across positive end-expiratory pressure levels after inflation from functional residual capacity, but peaked at moderate positive end-expiratory pressure after deflation from total lung capacity, further demonstrating the effects of volume history and providing experimental validation of the recruitment models of Hickling (*AJRCCM* 2001;163:69–78). These results support the interpretation of P_{flex} as pressure threshold for recruitment, but otherwise do not suggest a role for the pressure–volume curve in predicting steady-state lung volume.

Keywords: acute lung injury; computed tomography; mechanical ventilation; surfactant

Recruitment and maintenance of ventilated lung volume are essential for improving oxygenation in acute lung injury and the acute respiratory distress syndrome (ARDS) (1). The most commonly employed strategy to achieve this end is the use of positive end-expiratory pressure (PEEP), with or without the addition of sighs or periodic high inflation pressure recruitment maneuvers. Significant controversy persists over the optimal method for determining the amount of PEEP to apply. Some have suggested that PEEP be set on the basis of parameters derived from an inspiratory pressure–volume (P–V) curve and the presence of a slope change (P_{flex}) therein (2, 3), whereas the scheme used in the National Institutes of Health ARDS Network low V_T ventilation trial was a simple PEEP–F_IO₂ (fractional inspired oxygen concentration) ladder (4). Others have advocated finding optimal PEEP by reducing PEEP in steps from a high level until the arterial partial pressure of oxygen

(Pa_{O₂}) falls below a prescribed level, and then rerecruiting the lung and adjusting PEEP to a level just above that at which the fall occurred (5), or finding the PEEP that yields the maximal tidal compliance after a recruiting maneuver (6).

Originally, the rationale behind the use of the inspiratory P–V curve to guide ventilator settings was that the shape of the curve, in particular the increasing slope or compliance above P_{flex}, reflected the recruitment of poorly ventilated lung regions and that the flattening of the curve at higher pressures reflected overdistension (2, 3). More recent data suggest that recruitment actually occurs progressively and continuously along the curve above P_{flex} (5, 7–10). However, animal studies and models of acute lung injury have demonstrated that volume history is an important determinant of end-expiratory volume and, further, that steady-state lung volume during tidal ventilation may not reflect that seen in a static or quasi-static P–V curve (5, 6). Therefore, we sought to examine the relationship between steady-state lung volume and cumulative cyclic recruitment or derecruitment to the quasi-static P–V curve, using the saline lavage model of acute lung injury in anesthetized dogs. We looked at changes in end-expiratory volume over short time periods, as functions of volume history and end-expiratory pressure, by monitoring the cumulative changes in lung volume of small tidal loops. We also compared lung volume during steady-state mechanical ventilation, measured by computed tomography (CT) imaging, with the volume predicted by the P–V curve. Some of the results of these studies have been previously reported in abstract form (11, 12).

METHODS

Procedures were approved by the Institutional Animal Care and Use Committee (*see* the online supplement for additional details). Six dogs were anesthetized, intubated, and volume ventilated at an F_IO₂ of 1.0 and a rate of 15 breaths/minute. V_Ts (10–12 ml/kg) were adjusted to an end-tidal P_{CO₂} (P_{ETCO₂}) of 30–35 mm Hg and maintained thereafter. Airway pressure (P_{aw}), esophageal pressure (P_{es}), arterial blood pressure (Pa), P_{ETCO₂}, and oxygen saturation (Sa_{O₂}) were continuously measured and recorded.

Lung Injury

Acute lung injury was induced by repeated lavage with warmed saline (60 ml/kg), repeated every 10 minutes while shifting each dog from the prone to the supine position, until the Pa_{O₂} fell below 90 mm Hg for 30 minutes.

P–V Curves

A computer-controlled system (*see* the online supplement) generated quasi-static P–V curves at constant flow (3 L/minute) over a preprogrammed range of pressures. P_{aw}, P_{es}, and flow signals were digitized and stored, allowing measurement of cumulative lung volume change from FRC over several cycles. The same P–V curve series were obtained before and after lavage injury. Vital capacity P–V curves were measured from 0 to 40 to 0 cm H₂O P_{aw} for three cycles. Curves were fit to the model of Venegas and coworkers (13), using the point of maximal compliance increase to define P_{flex}. Two series of tidal P–V loops with different volume histories were performed. Series 1 recorded three 10-cm H₂O amplitude tidal P–V loops over different pressure ranges after inflation from FRC, whereas Series 2 recorded the same series of

(Received in original form May 6, 2003; accepted in final form February 2, 2004)

Supported by National Institutes of Health grant HL58504.

Present affiliation of J.M.D.: Department of Pediatrics, University of Chicago, Chicago, Illinois.

Correspondence and requests for reprints should be addressed to Brett A. Simon, M.D., Ph.D., Department of Anesthesia, Tower 711, Johns Hopkins Hospital, Baltimore, MD 21287-8711. E-mail: bsimon@jhmi.edu

This article has an online supplement, which is accessible from this issue's table of contents online at <http://www.atsjournals.org>

Am J Respir Crit Care Med Vol 169, pp 957–962, 2004

Originally Published in Press as DOI: 10.1164/rccm.200305-6140C on February 5, 2004

Internet address: www.atsjournals.org

loops after deflation from total lung capacity (TLC, defined as 40 cm H₂O Paw). For both, loops were performed over incrementally increasing pressures from 0 to 40 cm H₂O (i.e., 0–10, 5–15, 10–20...30–40 cm H₂O). Five to 10 minutes of tidal ventilation was resumed between measurements, until P_{ET}CO₂ returned to normal.

CT Imaging

Five dogs were prepared as described above and underwent supine whole-lung CT imaging before and after lavage for measurement of steady-state air volumes over a range of PEEP values. Contiguous 10-mm images were obtained with a GE 9800 scanner (General Electric, Fairfield, CT) during steady-state mechanical ventilation gated to end expiration, one image per breath, with incremental table movement between images. Ventilation was not held or interrupted for imaging. Imaging was repeated at 0 (FRC), 5, 10, 15, and 20 cm H₂O PEEP, with a 10-minute equilibration period after each PEEP change. Vital capacity quasi-static P–V curves were obtained as described above before imaging.

Images were analyzed using NIH Image (<http://rsb.info.nih.gov/nih-image>) on a Macintosh computer. Images were calibrated against the measured density of air and tissue from each image set to quantify density as “percent air.” The lung tissue in each slice was manually outlined and the air and tissue volumes were calculated from the product of lung area, slice thickness, and density. The individual slice volumes were summed to give total, tissue, and air volume, which was plotted against PEEP to generate “CT P–V curves” representing the end-expiratory volumes of the lung during steady-state ventilation. The air CT P–V curve was plotted alongside the quasi-static curve, assuming that the CT measured lung volume at FRC corresponded to the initial lung volume for the quasi-static P–V curve.

Statistical Analysis

Values are reported as means ± SEM. A paired Student’s *t*-test was used to assess differences in ΔV and specific compliance (sC) (StatView 4.5; SAS Institute, Cary, NC). Statistical significance was accepted at *p* < 0.05.

RESULTS

Lung lavage resulted in a significant decrease in oxygenation, with arterial P_O₂ falling from 496 ± 24 mm Hg in control animals to 85 ± 5 mm Hg 30 minutes after lavage. The control vital capacity P–V curves exhibited the classic sigmoid shape with minimal hysteresis. Whereas the first inspiratory curve frequently showed lower volumes and initial compliance, particularly at lower pressures, than subsequent loops, the descending curve and the second and third loops were generally superimposable (Figure 1, *top*). After lavage, the curves exhibited increased hysteresis and a change in compliance in the midinflation limb, allowing identification of a clear P_{flex} (Figure 1, *bottom*). P_{flex} was evident whether the Paw (19.9 ± 2.7 cm H₂O) or transpulmonary pressure (P_{tp}) (17.8 ± 2.6 cm H₂O) pressure was used.

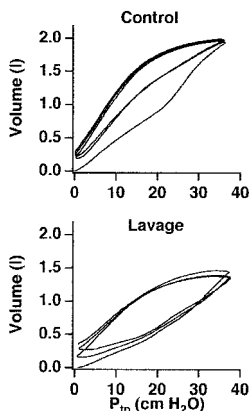


Figure 1. Vital capacity pressure–volume (P–V) curves from representative animal before and after saline lavage injury. Total lung capacity was defined at an airway pressure of 40 cm H₂O, which resulted in a slightly lower maximum transpulmonary pressure (P_{tp}).

Frequently, the first inflation loop was different from the subsequent two, suggesting some recruitment attained in the first loop was maintained for subsequent loops. Vital capacity, defined as the volume of the P–V curve from 0 to 40 cm H₂O Paw, fell 17 ± 4% after lavage (mean control VC was 1.39 ± 0.16 L).

In the control series, tidal loops from FRC were narrow and remained close to the envelope P–V curve except over the upper third of the pressure range, where they became more parallel to the pressure axis. On deflation from TLC the tidal loops were close to the deflation limb P–V curve over the entire pressure range (Figure 2). Tidal loops after lavage changed considerably from control. Loops from FRC tended to remain close to the ascending P–V curve at low pressures with a small amount of tidal recruitment. However, when the peak tidal loop pressure exceeded P_{flex}, the tidal recruitment per loop greatly increased (Figure 3). Loops performed after deflation from TLC had greater hysteresis area than controls and were generally parallel to the deflation P–V curve, although at the lowest pressure ranges the slope of the loops dropped off (Figure 3).

Tidal recruitment (ΔV) during tidal P–V loops was defined as half the increase in end-expiratory volume over the second and third tidal loops (Figure 4). This definition avoids including volume changes from deflation hysteresis. Loop compliance was determined from the difference between the starting (end-expiratory) and peak (end-inspiratory) lung volumes during the second tidal loop, divided by the 10-cm H₂O pressure difference. Loop compliance was normalized to control vital capacity for each animal to give specific compliance (sC) to facilitate combining results from different-sized animals for statistical analysis.

Quantification of tidal recruitment (Figure 5) shows that, after inflation from FRC, the volume recruited in the lavaged lungs becomes significantly greater than in the control lungs (*p* < 0.05) when the peak loop airway pressure exceeds P_{flex} (Figure 5). In fact, at the lowest pressure range control recruitment was significantly greater than lavage recruitment, reflecting the higher opening pressures needed to recruit the lavaged lung. Deflation limb recruitment was less than inflation limb recruitment, and was significantly different between control and lavage at the lowest pressure range (control greater) and the highest pressure range (lavage greater) (Figure 5).

Specific compliance of control tidal loops was maximal at low pressure ranges and decreased as pressure increased for both inflation and deflation series (Figure 6). In contrast, sC in the lavage lung after inflation from FRC was low and changed only slightly over the entire range. After deflation from TLC, however, sC changed twofold over the range of pressures, reaching a maximum at a PEEP of 10 cm H₂O (Figure 6). Note these data are plotted against minimum loop pressure (PEEP) for comparison with the literature (see below); midcycle Paw and peak Paw are 5 and 10 cm H₂O greater, respectively.

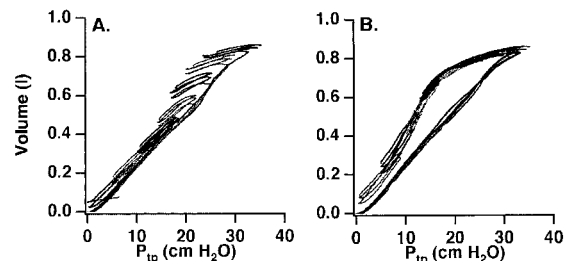


Figure 2. Composite tidal P–V loops from a representative control condition after inflation from FRC (A) or deflation from TLC (B). Individual loops for each separate tidal P–V run with their volume histories are superimposed on the same axes.

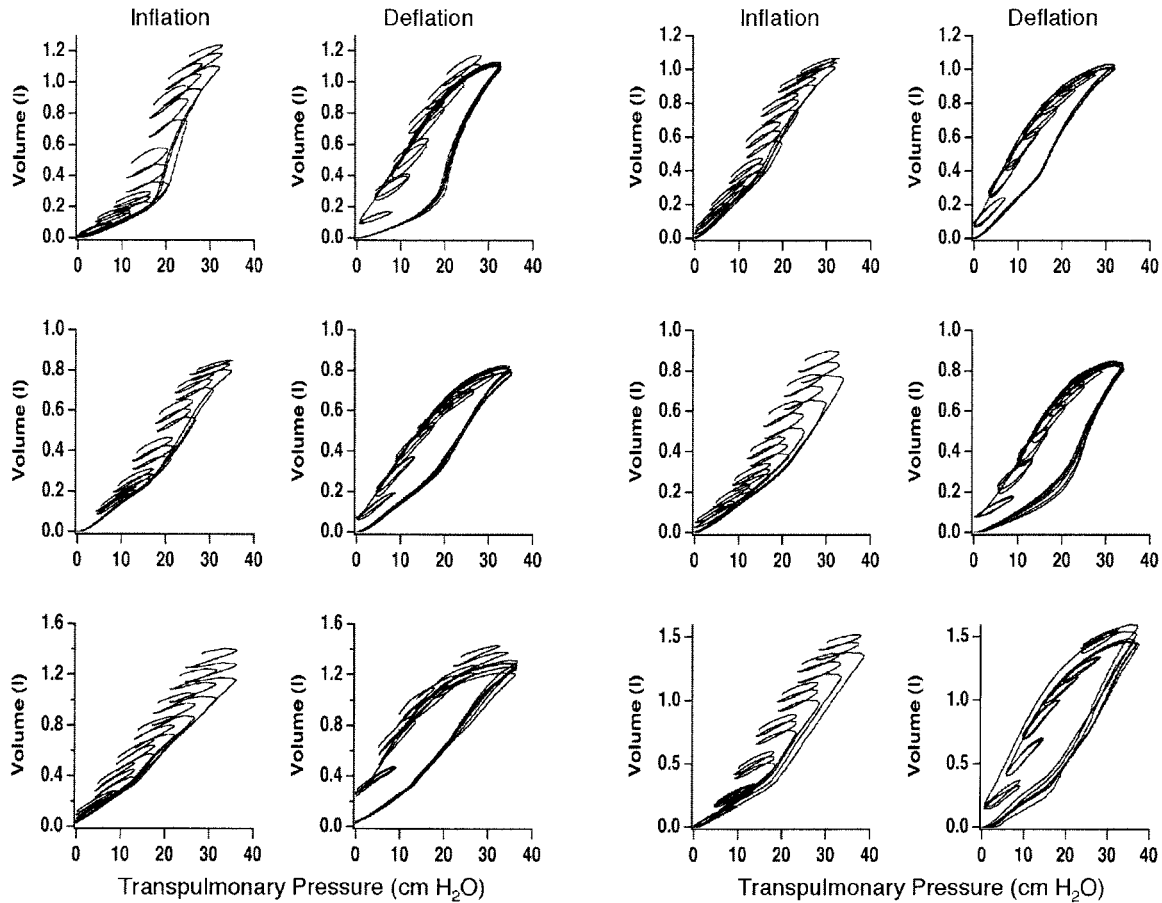


Figure 3. Composite tidal P–V loops for six animals postlavage lung injury after inflation from FRC or deflation from TLC. Individual loops for each separate tidal P–V run with their volume histories are superimposed on the same axes.

Quasi-static and CT P–V curves for five dogs were normalized to each lung’s quasi-static curve TLC, averaged, and plotted on the same axes with the assumption that the lung volumes were equal at FRC (Figure 7). P_{flex}, obtainable for four of the five quasi-static P–V curves, was equal to 15.3 ± 2.4 cm H₂O. Peak inspiratory airway pressures during CT imaging averaged 19 ± 1.8 , 20 ± 2.3 , 24 ± 1.5 , 33 ± 3.2 , and 44 ± 2.9 at 0, 5, 10, 15, and 20 cm H₂O PEEP, respectively, at an average V_T of 260 ± 14.1 ml. The steady-state end-expiratory lung volume, as defined by the CT data, was not related in any obvious way to the quasi-static P–V curve. Lung volume was underestimated at all PEEP levels by the inflation P–V curve. The deflation P–V curve over-

estimated lung volume at low PEEP and underestimated it at high PEEP. It is important to note that at the 10- to 12-ml/kg V_Ts used for these CT studies, peak inspiratory pressures were greater than the 10-cm H₂O increments used in the tidal loop studies, exceeding 40 cm H₂O at the highest PEEP level. The mean end-inspiratory pressures and volumes during CT imaging at each PEEP, estimated by adding the peak inspiratory pressure to the PEEP and the set V_T to the CT lung air volume, are presented as open circles in the same figure (Figure 7). These tidal P–V trajectories appear to bear little relationship to the quasi-static P–V curve.

To present the air/tissue-partitioned CT P–V curves, the data

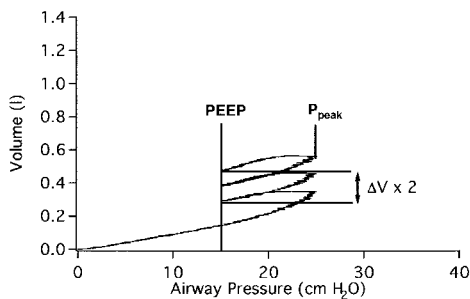


Figure 4. Example of three tidal P–V loops over the airway pressure range of 15 to 25 cm H₂O after inflation from FRC. ΔV = tidal recruitment per breath measured over second and third tidal loops; PEEP = positive end-expiratory pressure; P_{peak} = peak airway pressure.

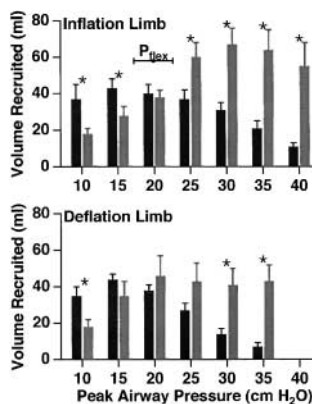


Figure 5. Tidal recruitment per breath (ΔV) data from all six animals (before (solid columns) and after (gray columns) lavage lung injury for tidal loops performed after inflation from FRC or deflation from TLC. Data are plotted against P_{peak} for the cycle to highlight the role of P_{flex} as a pressure threshold for recruitment. P_{flex} was determined by curve fitting each animal’s vital capacity P–V curve, using the method of Venegas and co-workers (13). Data represent means \pm SEM; *p < 0.05, injured versus control.

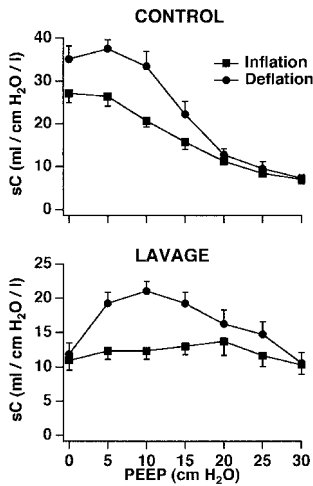


Figure 6. Specific compliance (sC) data for tidal loops from all animals before (*control*) and after lavage lung injury (*lavage*) for tidal loops performed after inflation from FRC or deflation from TLC. These data are plotted as functions of minimum loop pressure (PEEP) for comparison with the model data of Hickling (6). Data represent means \pm SEM.

for each animal were normalized to the total (air plus tissue) volume at 20 cm H₂O PEEP in the control condition, and then averaged (Figure 8). Because this total lung volume is greater than the TLC air volume used to normalize the data in Figure 7, the resulting normalized air volumes in Figure 8 are lower but allow direct comparison of how the air and tissue volume components change with injury and incremental PEEP. Tissue volume at FRC increased from 12.4 \pm 1.0% under control conditions to 22.5 \pm 1.5% after lavage, and the tissue volume changed less than 1% over the range of PEEPs, indicating minimal change in intrapulmonary blood volume and/or clearance of edema fluid from the lung with increasing PEEP. Total lung volume was unchanged after lavage, suggesting that the loss of air volume with injury was due to flooding rather than collapse or atelectasis because the reduction in air volume was offset by an equal increase in tissue volume.

DISCUSSION

The optimal management of mechanical ventilation during acute lung injury depends on the recruitment and maintenance of ventilated lung volume, balancing end-inspiratory recruitment with overdistension while also balancing end-expiratory derecruitment with the reduced V_Ts and hemodynamic consequences of PEEP. The changed shape of the inspiratory P-V curve in lung injury, with an increased and linear compliance between a lower and upper P_{flex}, was interpreted to represent a range of pressures over which the lung could be ventilated without derecruitment or overdistension (2, 3). Many subsequent animal (5) and human (8-10) studies have suggested that recruitment occurs progressively and continuously above P_{flex} and, further, that steady-state lung volume during tidal ventilation may not reflect that seen in the P-V curve. Hickling used a simple mathematical model of the ARDS lung to elegantly show how this could be

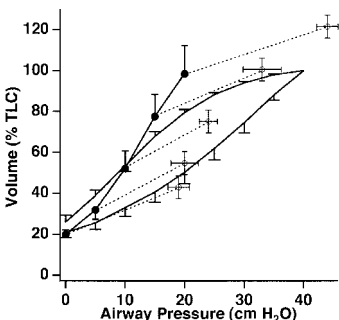


Figure 7. Quasi-static (solid line) and CT-derived (solid circles) P-V curves for five lavage-injured dogs, superimposed with the assumption that volumes are equal at FRC. Open circles estimate end-inspiratory pressure and volume during CT imaging based on peak inspiratory pressure and set V_T. Data represent means \pm SEM.

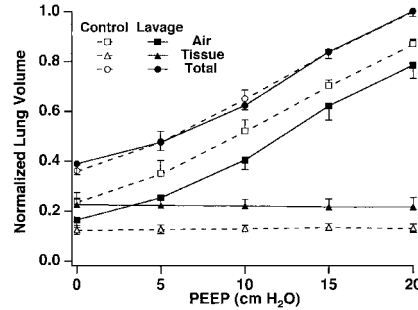


Figure 8. Whole-lung CT P-V curves partitioned into total, air, and “tissue” volumes for the five animals of Figure 7 before and after lavage injury. Data represent means \pm SEM.

so (7), and then went on to predict that tidal compliance and end-expiratory volume will depend on both the volume history and V_T applied (6). Our data provide experimental confirmation of these model predictions of Hickling, emphasizing the importance of short-term volume history in the recruitment behavior of the lung and the interpretation of P_{flex} as a threshold for end-inspiratory tidal recruitment. These data further indicate that the steady-state end-expiratory lung volume is not predicted by the quasi-static P-V curve.

Experimental Considerations

We chose the saline lavage model of acute lung injury for these studies, a commonly employed model of surfactant depletion and alveolar edema known for its consistency and stability (14, 15). Whole lung P-V curves performed before and after our 1- to 2-hour tidal curve protocol were minimally changed, demonstrating the stability of the preparation despite the large V_T ventilation and repeated vital capacity inflations. This stability is evident in the overlapping inflation and deflation P-V trajectories seen as superimposed volume histories for the repeated individual P-V loop measurements in Figure 3. Compared with other lung injury models such as oleic acid, the lavage model may be considered to be highly recruitable, achieving close to full preinjury lung volume at TLC (12, 16). Although surfactant inactivation is an important component of lung mechanical dysfunction in clinical acute lung injury (17), the relevance of these results to the human condition may vary depending on the degree of mechanical similarity of an individual’s lung injury to this model.

Obtaining safe, consistent and repeatable P-V curves in injured lungs is difficult (18), and many attempts have been made to automate this process to improve speed, safety, and reliability (19-22). Although resistive losses may cause small differences between results obtained by static methods, in which the lung is permitted to reach an equilibrium pressure at each volume step, and quasi-static methods, in which pressure and volume are measured continuously during a steady inflation and deflation of the lung, these differences are minimal at low flow rates and are more than offset by the technical difficulties in determining stable plateau pressures in the injured lung. At a steady flow of 3 L/minute, neither expiratory flow limitation nor auto-PEEP should have been significant (23-25). Our computer-controlled system (see the online supplement) has the advantage of continuously tracking cumulative changes in volume over several programmed inflation/deflation cycles, allowing measurement of incremental recruitment. The system was tested for leaks by confirming conservation of volume with repeated cycling of a rubber bag (see Figure E1 in the online supplement) and by clamping the endotracheal tube at end inspiration and checking for maintenance of airway pressure for 20 seconds. We did not correct for differences between O₂ consumption and CO₂ production, which we estimate to be less than 2.3 ml for a tidal loop and 20 ml for a vital capacity curve (see the online supplement for

details). We did, however, correct for gas compression, because measurements are made over a wide range of airway pressures. Finally, we chose to use the average recruitment over the second and third tidal loops as our measure of recruitment, avoiding attributing the difference in inflation and deflation limb hysteresis volume to V_T recruitment. We limited the tidal P–V data acquisition to three cycles as a trade-off between reasonable time for each protocol, potential hypoxemia and hypercarbia with reduced ventilation in the injured lung, and additional information available from added cycles. In pilot studies we found that although inspiratory tidal recruitment frequently continued beyond 3 cycles, it generally reached a plateau after 6–10 cycles.

Vital Capacity P–V Curves

Vital capacity P–V curves showed the expected change in shape after lung injury, with moderate reduction in vital capacity, increased hysteresis, and a change in slope in the midinflation limb identified as Pflex (Figure 1). Of note, after disconnecting the circuit and deflation to FRC there was commonly a difference between the first and subsequent inflation curves under control conditions, demonstrating that even in the normal lung there can be some lung derecruitment, units with elevated opening pressures that recruit and remain open with a subsequent deflation to zero pressure. This dependence on volume history, even in uninjured lungs, underscores the importance of standardized conditions in interpreting P–V data in the clinical setting. We inflated the lungs to a maximum Paw of 40 cm H₂O, corresponding to a Ptp of 33–36 cm H₂O, and although there was frequently a slight decrease in slope at the top of the inflation curve (Figure 3) no upper Pflex or plateau was identified. Although a plateau may have been identified with inflation to higher pressures, we choose a maximum Paw of 40 cm H₂O as a compromise to preserve the stability of the preparation.

Tidal P–V Loops

Control tidal P–V loops from FRC remained parallel to the inflation P–V curve until a relatively high peak lung volume was attained (Figure 2). Because there appeared to be minimal recruitment with each cycle, the change in slope (which was similar for inflation and deflation of the loops) may reflect reduced surface tension from the increased presence of surface active molecules at the air–liquid interface of alveoli and small airways after an increase in surface area (26), the normal hysteresis behavior of the lung. After lavage injury, however, there was clearly volume recruitment with each cycle in which the peak pressure exceeds Pflex (Figure 3). The first cycle of the inflation limb data (Figure 3) closely resembles the predictions of Hickling (6 [Figures 2 and 3]), in which the compliance change is entirely attributable to recruitment phenomena. Subsequent tidal increases in volume reflect additional recruitment not included in Hickling's model. As predicted by the model (6) and as demonstrated by our data and several studies (9, 10, 27–29), recruitment occurred all the way up to TLC. Pflex may thus be interpreted as a pressure threshold for recruitment: when peak inspiratory pressure exceeds Pflex, incremental volume recruitment occurs (Figure 5).

Deflation limb tidal loops lie close to the P–V envelope, with little tidal recruitment (Figures 3 and 5). A statistically significant difference in deflation limb recruited volume between control and injured lungs occurred at the lowest tidal range, with the injured lung exhibiting less recruitment, and the highest two ranges, with the injured lung recruiting more volume. This difference likely reflects the rapid derecruitment of the lavaged lung and inability to rerecruit with peak inspiratory pressure less than Pflex. Similar to the predictions of Hickling (6), the slope of the tidal loop became less than the deflation P–V limb only at low PEEP values, again reflecting end-expiratory alveolar collapse with resultant lower ventilated volume and lower compliance.

In control lungs, specific compliance (sC) of tidal loops fell with increasing PEEP (Figure 6), indicating the lungs became stiffer as they were more inflated. In addition, sC was higher after deflation from TLC than on the inflation limb (Figure 7). As discussed above, the higher deflation sC values may reflect recruitment and larger lung volumes or, more likely in these normal lungs, the effect of surfactant physiology (26). Note that these data were normalized to control condition vital capacity to facilitate combining data from different animals. Thus, this specific compliance parameter is not a measure of intrinsic lung mechanical properties because it is not normalized to the actual ventilated volume at the time of each measurement. sC behavior of the injured lung was considerably different. sC was relatively uniform along the inflation limb, whereas it varied more than twofold on the deflation limb, peaking at moderate PEEP well below Pflex (Figure 7). Again, these data provide strong experimental support of the models of Hickling (6), implemented at low V_T , and suggest that the whole lung compliance in acute lung injury is significantly influenced by tidal recruitment and derecruitment.

CT Image Data

The lung volumes measured by CT imaging reflect a steady-state equilibrium between end-inspiratory recruitment and end-expiratory derecruitment obtained after incremental PEEP increases, in contrast to the transient or nonequilibrium volumes obtained during a P–V curve. These steady-state lung volumes exceeded those on the inspiratory P–V curve for all pressures, and also exceeded the volumes on the deflation limb at higher PEEP levels. At the relatively large tidal volumes used (chosen to reduce hypercapnia during imaging because of the slow maximum imaging rate of the CT scanner), the peak inflation pressures were greater than Pflex for all PEEPs. Thus, the elevation of end-expiratory volume above the inspiratory P–V curve would be expected because of the effect of recruitment, as modeled by Hickling (6), with an additional contribution from the cumulative tidal recruitment demonstrated by the tidal P–V loops. At the highest PEEP levels the peak inflation pressures slightly exceeded the 40-cm H₂O limit of the P–V curve, so the additional recruitment thus obtained caused the end-expiratory volumes to break out of the P–V envelope, an effect also predicted by Hickling's model (6). It is important to underscore that these CT data do not look at the time course of changes after a recruitment maneuver, but rather the net effect of recruitment and derecruitment after an increment in PEEP in a relatively short (10- to 20-minute) time frame. Similar results, in which the CT-determined lung volume was monitored after a recruitment maneuver in lavage injured dogs, were reported by Lim and coworkers, with total lung air volumes continuing to increase for 30 minutes after a PEEP increase compared with only small additional increases over time after a recruitment maneuver (30).

Air/Tissue Partitioned CT P–V Curves

Partitioning of the CT P–V curves into air, “tissue” (which includes all components of approximately water density such as blood, edema, and cells), and total (air plus tissue) volumes adds an additional perspective on the nature of steady-state lung recruitment in the lavage model. First, total lung volumes before and after lavage are approximately equal, suggesting that the loss of air volume with injury is primarily due to flooding because of the offsetting changes in air and tissue volumes, consistent with observations made in oleic acid-injured lungs using the parenchymal marker technique (31). Atelectasis or airspace collapse would show up as a loss of total lung volume compared with control in this analysis, although one cannot rule out regional atelectasis with equally offsetting air trapping at FRC as an alternative explanation. Second, the tissue volume remained constant as PEEP increased, suggesting that the total amount of edema (including residual lavage fluid) was constant over

time and, further, that intrapulmonary blood volume did not change with increasing PEEP. Thus, as the lung is recruited this fluid volume must be redistributed and relocated within the lung. Further studies of the changes in regional lung volume and density with inflation and recruitment, combined with whole lung analysis such as this, are needed to better understand the local phenomena of lung recruitment in different injury models and patients.

Conclusions

Small-volume tidal P-V loops performed after inflation from FRC in the lavage-injured lung demonstrated incremental, cyclic recruitment if the peak pressure achieved exceeded P_{flex} on the vital capacity quasi-static P-V curve, whereas loops performed after deflation from TLC remained close to the envelope deflation P-V curve. Recruitment continued to occur up to and beyond a peak inspiratory airway pressure of 40 cm H₂O, as demonstrated by both the tidal loops and the steady-state large V_T CT-derived lung volume data. Tidal-specific compliance was relatively constant across PEEP levels after inflation from FRC, but peaked at moderate PEEP after deflation from TLC, further demonstrating the effects of volume history and providing experimental validation of the recruitment models of Hickling (6, 7). These results support the interpretation of P_{flex} as pressure threshold for recruitment, but otherwise do not suggest a role for the pressure-volume curve in predicting steady-state lung volume.

Conflict of Interest Statement: J.M.D. has no declared conflict of interest; A.J.N. has no declared conflict of interest; B.A.S. has no declared conflict of interest.

Acknowledgment: The authors thank Vince Lerie for technical support with the CT scanner, Matt Piper for assistance in the laboratory, and Respironics (Murraysville, PA) for providing the modified PLV-102 ventilator.

References

- Lachmann B. Open up the lung and keep the lung open [editorial; comment]. *Intensive Care Med* 1992;18:319-321.
- Roupie E, Dambrosio M, Servillo G, Mentec H, el Atrous S, Beydon L, Brun-Buisson C, Lemaire F, Brochard L. Titration of tidal volume and induced hypercapnia in acute respiratory distress syndrome. *Am J Respir Crit Care Med* 1995;152:121-128.
- Amato MB, Barbas CS, Medeiros DM, Magaldi RB, Schettino GP, Lorenzi-Filho G, Kairalla RA, Deheinzelin D, Munoz C, Oliveira R, et al. Effect of a protective-ventilation strategy on mortality in the acute respiratory distress syndrome. *N Engl J Med* 1998;338:347-354.
- Brower RG, Matthay MA, Morris A, Schoenfeld D, Thompson BT, ARDS Network. Ventilation with lower tidal volumes as compared with traditional tidal volumes for acute lung injury and the acute respiratory distress syndrome. *N Engl J Med* 2000;342:1301-1308.
- Rimensberger PC, Cox PN, Frndova H, Bryan AC. The open lung during small tidal volume ventilation: concepts of recruitment and "optimal" positive end-expiratory pressure. *Crit Care Med* 1999;27:1946-1952.
- Hickling KG. Best compliance during a decremental, but not incremental, positive end-expiratory pressure trial is related to open-lung positive end-expiratory pressure: a mathematical model of acute respiratory distress syndrome lungs. *Am J Respir Crit Care Med* 2001;163:69-78.
- Hickling KG. The pressure-volume curve is greatly modified by recruitment: a mathematical model of ARDS lungs. *Am J Respir Crit Care Med* 1998;158:194-202.
- Svantesson C, Sigurdsson S, Larsson A, Jonson B. Effects of recruitment of collapsed lung units on the elastic pressure-volume relationship in anaesthetized healthy adults. *Acta Anaesthesiol Scand* 1998;42:1149-1156.
- Richard JC, Brochard L, Vandelet P, Breton L, Maggiore SM, Jonson B, Clabault K, Leroy J, Bonmarchand G. Respective effects of end-expiratory and end-inspiratory pressures on alveolar recruitment in acute lung injury. *Crit Care Med* 2003;31:89-92.
- Jonson B, Richard JC, Straus C, Mancebo J, Lemaire F, Brochard L. Pressure-volume curves and compliance in acute lung injury: evidence of recruitment above the lower inflection point. *Am J Respir Crit Care Med* 1999;159:1172-1178.
- Downie JM, Simon BA. Pressure threshold for volume recruitment during tidal ventilation after lung lavage [abstract]. *Am J Respir Crit Care Med* 1999;161:A76.
- Simon BA, Marcucci C, Piper MG, Downie JM. CT P-V analysis differentiates flooding vs collapse in oleic acid (OA) and lavage injury models [abstract]. *Am J Respir Crit Care Med* 2000;161:A486.
- Venegas JG, Harris RS, Simon BA. A comprehensive equation for the pulmonary pressure-volume curve. *J Appl Physiol* 1998;84:389-395.
- Lichtwarck-Aschoff M, Hedlund AJ, Nordgren KA, Wegenius GA, Markstrom AM, Guttman J, Sjostrand UH. Variables used to set PEEP in the lung lavage model are poorly related. *Br J Anaesth* 1999;83:890-897.
- Lewis J, McCaig L, Hafner D, Spragg R, Veldhuizen R, Kerr C. Dosing and delivery of a recombinant surfactant in lung-injured adult sheep. *Am J Respir Crit Care Med* 1999;159:741-747.
- Kloot TE, Blanch L, Melyne Youngblood A, Weinert C, Adams AB, Marini JJ, Shapiro RS, Nahum A. Recruitment maneuvers in three experimental models of acute lung injury: effect on lung volume and gas exchange. *Am J Respir Crit Care Med* 2000;161:1485-1494.
- Lewis JF, Jobe AH. Surfactant and the adult respiratory distress syndrome. *Am Rev Respir Dis* 1993;147:218-233.
- Hudson LD. Protective ventilation for patients with acute respiratory distress syndrome. *N Engl J Med* 1998;338:385-387.
- Servillo G, De Robertis E, Maggiore S, Lemaire F, Brochard L, Tufano R. The upper inflection point of the pressure-volume curve: influence of methodology and of different modes of ventilation. *Intensive Care Med* 2002;28:842-849.
- Servillo G, Svantesson C, Beydon L, Roupie E, Brochard L, Lemaire F, Jonson B. Pressure-volume curves in acute respiratory failure: automated low flow inflation versus occlusion. *Am J Respir Crit Care Med* 1997;155:1629-1636.
- Lu Q, Vieira SR, Richecoeur J, Puybasset L, Kalfon P, Coriat P, Roubey JJ. A simple automated method for measuring pressure-volume curves during mechanical ventilation. *Am J Respir Crit Care Med* 1999;159:275-282.
- Kondili E, Prinianakis G, Hoeing S, Chatzakis G, Georgopoulos D. Low flow inflation pressure-time curve in patients with acute respiratory distress syndrome. *Intensive Care Med* 2000;26:1756-1763.
- Greville HW, Arnup ME, Mink SN. Density dependence of maximal flow is lung volume dependent during bronchoconstriction. *J Appl Physiol* 1987;62:691-705.
- Macklem PT, Mead J. Factors determining maximum expiratory flow in dogs. *J Appl Physiol* 1968;25:159-169.
- Vieillard-Baron A, Prin S, Schmitt JM, Augarde R, Page B, Beauchet A, Jardin F. Pressure-volume curves in acute respiratory distress syndrome: clinical demonstration of the influence of expiratory flow limitation on the initial slope. *Am J Respir Crit Care Med* 2002;165:1107-1112.
- Nunn JF. *Nunn's applied respiratory physiology*, 4th ed. Boston: Butterworths; 1993.
- Crotti S, Mascheroni D, Caironi P, Pelosi P, Ronzoni G, Mondino M, Marini JJ, Gattinoni L. Recruitment and derecruitment during acute respiratory failure: a clinical study. *Am J Respir Crit Care Med* 2001;164:131-140.
- Chelucci GL, Dall'Ava-Santucci J, Dhainaut JF, Chelucci A, Allegra A, Lockhart A, Zin WA, Milic-Emili J. Association of PEEP with two different inflation volumes in ARDS patients: effects on passive lung deflation and alveolar recruitment. *Intensive Care Med* 2000;26:870-877.
- Richard JC, Maggiore SM, Jonson B, Mancebo J, Lemaire F, Brochard L. Influence of tidal volume on alveolar recruitment: respective role of PEEP and a recruitment maneuver. *Am J Respir Crit Care Med* 2001;163:1609-1613.
- Lim CM, Soon Lee S, Seoung Lee J, Koh Y, Sun Shim T, Do Lee S, Sung Kim W, Kim DS, Dong Kim W. Morphometric effects of the recruitment maneuver on saline-lavaged canine lungs: a computed tomographic analysis. *Anesthesiology* 2003;99:71-80.
- Martynowicz MA, Minor TA, Walters BJ, Hubmayr RD. Regional expansion of oleic acid-injured lungs. *Am J Respir Crit Care Med* 1999;160:250-258.